Erbium–thulium interaction in broadband infrared luminescent silicon-rich silicon oxide

Se-Young Seo, Jung H. Shin, Byeong-Soo Bae, Namkyoo Park, J. J. Penninkhof et al.

Citation: Appl. Phys. Lett. **82**, 3445 (2003); doi: 10.1063/1.1577217
View online: http://dx.doi.org/10.1063/1.1577217
View Table of Contents: http://apl.aip.org/resource/1/APPLAB/v82/i20
Published by the American Institute of Physics.

Erbium–thulium interaction in broadband infrared luminescent silicon-rich silicon oxide

Se-Young Seo[a] and Jung H. Shin
Department of Physics, Korea Advanced Institute of Science and Technology (KAIST), 373-1 Kusung-dong, Yusung-gu, Taejon, Korea

Byeong-Soo Bae
Department of Materials Science and Engineering, Korea Advanced Institute of Science and Technology (KAIST), 373-1 Kusung-dong, Yusung-gu, Taejon, Korea

Namkyoo Park
Optical Communication Systems Laboratory, School of EECS, Seoul National University, Seoul 151-744, Korea

J. J. Penninkhof and A. Polman
FOM-Institute for Atomic and Molecular Physics (AMOLF), Kruislaan 407, 1098 SJ Amsterdam, The Netherlands

(Received 3 March 2003; accepted 24 March 2003)

The Er–Tm interaction and its effect on the luminescence from Er–Tm codoped silicon-rich silicon oxide (SRSO) is investigated. Er and Tm ions were implanted into SRSO films, which consist of Si nanocrystals embedded in a SiO_2 matrix. A broad luminescence spectrum extending from 1.5 to 2.0 μm was observed under excitation with a single light source due to the simultaneous, nonresonant excitation of both Er^{3+} and Tm^{3+} via Si nanocrystals. The absolute Er^{3+} luminescence intensity, however, is reduced relative to the case without Tm codoping. Comparison of the Er^{3+} and Tm^{3+} luminescence intensities, lifetimes, and their pump power dependence suggest that Er–Tm interaction leading to an energy transfer from the Er^{3+}:$^4I_{13/2}$ state to the excited Tm^{3+}:$^3H_4$ state is responsible for the reduction in the Er luminescence intensity. © *2003 American Institute of Physics.* [DOI: 10.1063/1.1577217]

The ever increasing optical information traffic is demanding broadband optical amplification beyond the conventional 1.5-μm window currently served by erbium-doped fiber amplifiers (EDFAs), in order to fully utilize the 1.4–1.7-μm low-loss band of silica-based optical fibers. A logical extension of EDFAs would be the addition of other rare-earth (RE) ions, such as Tm^{3+}, that luminesce in the desired wavelength range.[1] Such an approach, however, has the disadvantage of requiring separate pump lasers tuned to an absorption band of each doped RE ion, greatly increasing the complexity and the cost.

By using Si nanocrystals (nc-Si) as sensitizers, however, many different RE ions can be excited at once using a single pump source because nc-Si can excite RE ions nonresonantly via an Auger-type interaction with photogenerated excitons.[2–6] Such nc-Si sensitization also leads to a large effective excitation cross section for RE ions, thus requiring only a low-cost, broadband light source. Recently, we have observed optical gain in such nc-Si sensitized, Er-doped waveguides, demonstrating the feasibility of developing such nc-Si sensitized optical amplifiers.[7]

In this letter, we report on the Er and Tm luminescence and Er–Tm interaction in Er- and Tm-implanted silicon-rich silicon (SRSO) films that consist of nc-Si embedded in a SiO_2 matrix. We can observe broad luminescence from 1.5 to 1.9 μm due to simultaneous luminescence of both Er^{3+} and Tm^{3+}. The absolute Er luminescence intensity, however, is reduced relative to the case without Tm codoping. Based on a comparison of the Er^{3+} and Tm^{3+} luminescence intensities, lifetimes, and their pump power dependence, we identify Er–Tm interaction leading to energy transfer from the Er^{3+}:$^4I_{13/2}$ state to the Tm^{3+}:$^3H_4$ state to be responsible for the reduction in the luminescence intensity.

SRSO thin films with 38 at. % Si and 1-μm thickness were deposited by electron cyclotron resonance plasma-enhanced chemical vapor deposition of SiH_4 and O_2, followed by a rapid thermal anneal in an Ar environment at 950 °C for 5 min.[3] After deposition, one set of samples was implanted with either Er or Tm ions with energies of 300 and 750 keV to produce a 410-nm thin layer with a uniform RE concentration of 0.04 at. %. These will be referred to as *XX*L, with *XX* referring to the RE species. A similar set of samples, referred to as *XX*H, with a higher RE concentration of 0.08 at. % was also produced. Finally, an Er- and Tm-codoped sample (referred to as ErTmL) was produced by combining Er and Tm implantation. (0.04 at. % each) After irradiation, all films were again rapid thermal annealed at 950 °C for 5 min and hydrogenated by a 1-h anneal at 700 °C in a forming gas environment to remove and passivate implantation defects. Photoluminescence (PL) spectra were measured using a 1/4-m monochromator, long-wavelength enhanced InGaAs photodiode, and the lock-in technique at room temperature. Either the 477- or 488-nm line of an Ar ion laser was selected for optical pumping. Time-resolved RE PL decay traces were recorded using a digitizing oscilloscope.

Figure 1 shows the PL spectra, measured using 200 mW of the 477-nm pump light. The peaks near 1.54 and 1.75 μm

[a]Electronic mail: seyoungseo@mail.kaist.ac.kr

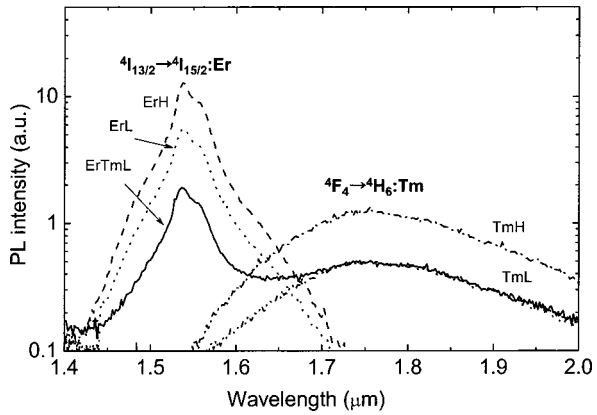

FIG. 1. PL spectra for Er- and/or Tm-implanted SRSO films. The sharp peaks at 1.54 μm and the relatively broad peaks around 1.75 μm are due to the $^4I_{13/2}\rightarrow{}^4I_{15/2}$ transition of Er^{3+} and the $^3F_4\rightarrow{}^3H_6$ transition of Tm^{3+}, respectively.

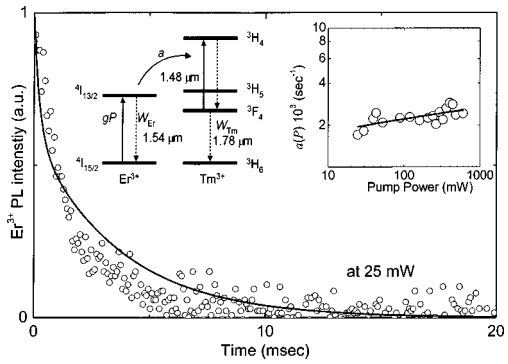

FIG. 3. Result of experiment (circles) and fit (solid line) of time-resolved Er^{3+} PL intensity at 1.54 μm for the ErTmL film measured upon 25-mW pump at 477 nm. The Er–Tm interaction model and the Er→Tm transfer rate a as a function of pump power are shown in the left and right insets, respectively.

are due to transition from the first excited state to the ground state of Er^{3+} ($^4I_{13/2}\rightarrow{}^4I_{15/2}$) and Tm^{3+} ($^3F_4\rightarrow{}^3H_6$), respectively. Since Tm:$^3H_4\rightarrow{}^3F_4$ transition occurs nonradiatively in silica-based materials, we could not observe ~1.45-μm Tm^{3+} luminescence attributed by such transition. For the ErL and TmL films, doubling the RE concentration doubles the RE PL intensities. Er and Tm codoping, however, significantly reduces the Er^{3+} PL intensity relative to the ErL film, but does not affect Tm^{3+} luminescence intensity.

A similar effect of Er–Tm codoping is observed on the luminescence lifetimes, as shown in Fig. 2. We find that the ErH and TmH films have the same RE luminescence decay traces as the ErL and TmL films, respectively. On the other hand, Er–Tm codoping results in a significant reduction of the Er^{3+} PL lifetime from 3.5 to 1.9 ms, while leaving the Tm^{3+} PL lifetime unaffected at 0.3 ms. Figure 1 demonstrates that with nc-Si sensitization and Er–Tm codoping, it is possible to obtain simultaneous luminescence of both Er^{3+} and Tm^{3+} using only a single light source, and thus possibly to obtain a very broad amplification window. However, for such amplification to be possible, the quenching of the Er^{3+} luminescence due to Tm codoping must be understood and controlled.

Since both the ErH and TmH films luminesce twice as strongly as the ErL and TmL films, respectively, and have

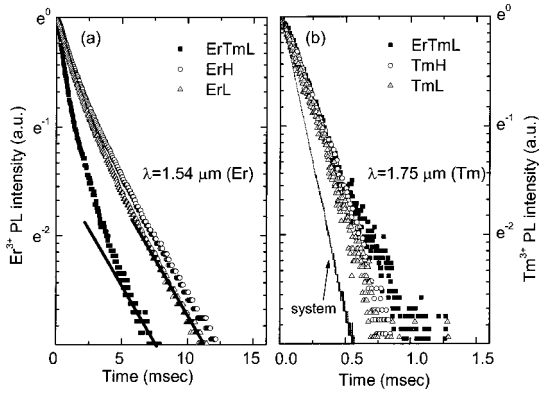

FIG. 2. Time-resolved decay traces Er^{3+} PL at 1.54 μm (a) and Tm^{3+} PL (b) at 1.78 μm. Data are shown for low (ErL,TmL) and high (ErH,TmH) concentrations, and for the codoped case (ErTmL). Two solid lines in (a) indicate typical decay traces with a lifetime of 4.5 ms.

nearly the same RE luminescence lifetimes, it unlikely that the higher overall RE concentration of the ErTmL film is quenching the Er^{3+} luminescence (e.g., due to higher implantation damage or concentration quenching). However, the fact that Tm codoping reduces both the Er^{3+} luminescence intensity and lifetime indicates that Tm codoping introduces nonradiative decay paths for excited Er^{3+} ions. We note, however, that the Er^{3+} luminescence decay rate from the ErTmL, after a rapid initial decay, approaches that from the ErL film [see Fig. 2(a)] indicating that the nonradiative decay paths introduced by Tm codoping disappear within a few ms after the pump beam is turned off. Such nonradiative decay paths is likely to be attributed by the excited Tm^{3+} ions, since the excited Tm^{3+} ions decay within $<$ms as shown in Fig. 2(b).

Such results, we propose, can be understood by a model in which the Er–Tm interaction is dominated by a cooperative upconversion process in which an excited Er^{3+} atom decays nonradiatively by exciting an excited Tm^{3+} ion from the $^3F_4$ to the $^3H_4$ state (see inset in Fig. 3). Indeed the Er^{3+}:$^4I_{13/2}\leftrightarrow{}^4I_{15/2}$ transition is nearly resonant with the Tm^{3+}:$^3H_4\leftrightarrow{}^3F_4$ transition, with an energy mismatch of only ~0.05 eV. In fact, 1.4–1.5-μm pumping has been used for such excited state absorption in Tm-doped fiber amplifiers.[8] We neglect the possible energy transfer from the Er^{3+}:$^4I_{13/2}$ state to the Tm^{3+}:$^3H_6$ state, since we do not observe any appreciable long tail in the Tm^{3+}:$^3F_4\rightarrow{}^3H_6$ luminescence decay trace that would indicate excitation via the much longer lived Er^{3+}:$^4I_{13/2}$ state, and also since the Tm^{3+}:$^3F_4\leftrightarrow{}^3H_6$ transition is much less resonant with the Er^{3+}:$^4I_{13/2}\leftrightarrow{}^4I_{15/2}$ transition, with an energy mismatch of ~0.1 eV. Finally, we approximate that after the energy transfer, the Tm^{3+} ions decay nonradiatively from the $^3H_4$ state back to the $^3F_4$ nearly instantaneously, since the strong multiphonon effects in silica are known to result in a nonradiative Tm:$^3H_4\rightarrow{}^3F_4$ transition at a rate much faster than the radiative decay rate.[9]

The population of excited Er^{3+} ions in the ErTmL film can then be described by

$$\frac{dN^*_{\mathrm{Er}}(P,t)}{dt} = gP[N - N^*_{\mathrm{Er}}(P)] - N^*_{\mathrm{Er}}(P)[W_{\mathrm{Er}}(P) + \alpha N^*_{\mathrm{Tm}}(P,t)], \quad (1)$$

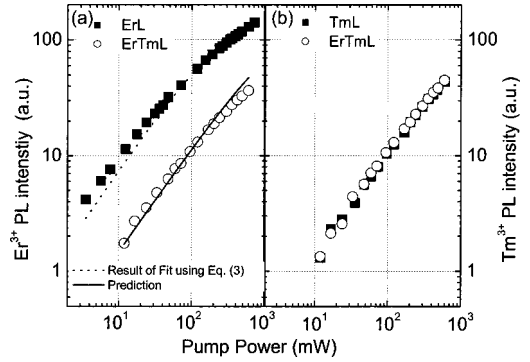

FIG. 4. Power dependence of Er^{3+} PL at 1.54 μm (a) and Tm^{3+} PL at 1.78 μm (b). Solid squares indicated data for the PL intensities implanted with Er or Tm only (ErL, TmL); open circles indicated co-implanted film.

where N, N_{Er}^{*} and N_{Tm}^{*}, g, and W_{Er} are the number density of optically active Er^{3+} ions, the number density of Er^{3+} and Tm^{3+} ions at the first excited state, the Er^{3+} excitation rate per pump power P, and Er^{3+} decay rate, respectively. α is the coupling coefficient between excited Er^{3+} and Tm^{3+} ions. Note that all parameters are dependent on P, except for N, g, and α.

As shown in Fig. 2, the time-resolved Tm^{3+} PL behaviors are well described by single-exponential decay with constant rate W_{Tm} independent of the presence of Er^{3+} ions. Thus, when the pump beam is turned off ($g=0$), $N_{\mathrm{Tm}}^{*}(t)$ decays as $N_{\mathrm{Tm}}^{*}(0)\exp(-W_{\mathrm{Tm}}t)$, allowing us to integrate Eq. (1) to obtain

$$N_{\mathrm{Er}}^{*}(t)=N_{\mathrm{Er}}^{*}(0)\exp\left(-\left\{W_{\mathrm{Er}}t+\frac{a}{W_{\mathrm{Tm}}}[1-\exp(-W_{\mathrm{Tm}}t)]\right\}\right), \tag{2}$$

where $a\equiv\alpha N_{\mathrm{Tm}}^{*}(0)$ represents the $Er^{3+}\rightarrow Tm^{3+}$ energy transfer rate, and is the only unknown value, since $W_{\mathrm{Er}}(P)$ and $W_{\mathrm{Tm}}(P)$ can be obtained experimentally. Figure 3 shows the result of fitting Eq. (2) to the Er^{3+} PL decay trace for the ErTmL sample, measured at a pump power of 25 mW, using only a as the fitting parameter. Despite the simplicity of the model, it describes the rapid initial decay followed by the long tail rather well. Additional decay measurements were made at different pump powers in the range from 25 to 600 mW. In all cases, similar fits were obtained. In this power range, the value of a increases slightly from 2×10^3 to 2.5×10^3 s^{-1}, as is shown in the inset of Fig. 3.

To confirm the validity of this energy transfer model, the pump power dependence of the Er^{3+} and Tm^{3+} intensities is investigated, as is shown in Fig. 4. We find that the Tm^{3+} PL intensity is unaffected by Er codoping at all pump powers [Fig. 4(b)], while the Er^{3+} PL intensity is quenched by Tm codoping at all pump powers [(Fig. 4(a)]. Note that both the Er^{3+} and the Tm^{3+} PL intensities from the ErTmL film increase nearly linearly as the pump power is increased from 25 to 600 mW. Thus, the relative intensity ratio changes only slightly, thereby explaining that a is nearly independent of pump power, as seen in the inset of Fig. 3. The slight increase in a with increasing pump power is attributed to the fact that the Er^{3+} PL intensity starts to saturate at a lower pump power than does the Tm^{3+} PL intensity.

In the steady state, $dN_{\mathrm{Er}}^{*}/dt=0$, and Eq. (1) can be rewritten for the ErL and ErTmL case:

$$I_{\mathrm{ErL}}^{\mathrm{Er}}=NW_R\frac{gP}{gP+W_{\mathrm{Er}}(P)},$$

$$I_{\mathrm{ErTmL}}^{\mathrm{Er}}=NW_R\frac{gP}{gP+W_{\mathrm{Er}}(P)+a(P)}, \tag{3}$$

where W_R is the Er^{3+} radiative decay rate. Now, in our model, the values related to Er such as g, N, W_R, and W_{Er} should be the same for both the ErL and ErTmL films. Thus, by measuring $I_{\mathrm{ErL}}^{\mathrm{Er}}$ and using the values of $a(P)$ derived from fitting the lifetime data (Fig. 3), it should be possible to predict $I_{\mathrm{ErTmL}}^{\mathrm{Er}}$. The dotted line in Fig. 4(a) is the result of fitting Eq. (3) to $I_{\mathrm{ErL}}^{\mathrm{Er}}$, and the solid line is the prediction for $I_{\mathrm{ErTmL}}^{\mathrm{Er}}$ using the values of NW_R and g (1.5×10^3 J^{-1}) found from the fit and the values of $a(P)$ found in Fig. 3. We find a good fit for $I_{\mathrm{ErL}}^{\mathrm{Er}}$, and more importantly, an excellent agreement between the predicted and measured values of $I_{\mathrm{ErTmL}}^{\mathrm{Er}}$ *even though the prediction had no adjustable parameters at all*, which strongly supports the validity of our proposed energy transfer model.

For broadband amplifier applications, such Er–Tm energy transfer reduces the efficiency, and therefore must be reduced. In the case of nc-Si sensitization, however, it will always be present if Er and Tm are codoped homogeneously, since Er^{3+} and Tm^{3+} ions are excited at the same time. Thus, the results presented in this letter indicate that for Er–Tm codoping to be successful, the film structure must be engineered on a nanometer scale, so that Er and Tm ions are separated sufficiently to suppress the energy transfer while still maintaining sufficient overall homogeneity for efficient wideband amplification.

In conclusion, we demonstrated broad 1.4–2.0-μm luminescence from Er–Tm codoped silicon-rich silicon oxide films using a single pump source. The Er^{3+} luminescence intensity and lifetime are significantly quenched by Tm codoping, while the Tm luminescence is not affected by the presence of Er. Based on the results, we propose that energy transfer from the Er^{3+}:$^4I_{13/2}$ state to excited Tm^{3+}:$^3H_4$ state is responsible for the observed Er^{3+} luminescence quenching, and that this transfer must be controlled if Er–Tm codoping is to be used for wideband optical amplification.

This work was supported in part by the NRL project, the National Nuclear Technology Program, the Fifth Leader Technology Development Project, and by BK 21 Project. The work at AMOLF is part of the research program of the FOM and was financially supported by NWO.

[1] J. Kani and M. Jinno, Electron. Lett. **35**, 1004 (1999).
[2] M. Fujii, M. Yoshida, Y. Kanazawa, S. Hayashi, and K. Yamanoto, Appl. Phys. Lett. **71**, 1198 (1997).
[3] J. H. Shin, M. Kim, S. Seo, and C. Lee, Appl. Phys. Lett. **72**, 1092 (1998).
[4] P. G. Kik, M. L. Brongersma, and A. Polman, Appl. Phys. Lett. **76**, 2325 (2000).
[5] G. Franzò, V. Vinciguerra, and F. Priolo, Appl. Phys. A: Mater. Sci. Process. **69**, 3 (1999).
[6] K. Watanabe, H. Tamaoka, M. Fujii, and S. Hayashi, J. Appl. Phys. **92**, 4001 (2002).
[7] H. Han, S. Seo, J. H. Shin, and N. Park, Appl. Phys. Lett. **81**, 3720 (2002).
[8] F. Roy, D. Bayart, A. L. Sauze, and P. Baniel, IEEE Photonics Technol. Lett. **13**, 788 (2001).
[9] E. R. Taylor, L. N. Ng, N. P. Sessons, and H. Buerger, J. Appl. Phys. **92**, 112 (2002).